

Interferometric terahertz imaging for detection of lethal agents using artificial neural network analyses

Aparajita Bandyopadhyay, Alexander M Sinyukov,
Amartya Sengupta, Dale E Gary and John F Federici
Dept of Physics, New Jersey Institute of Technology,
Newark, New Jersey 07103, United States of America,
Address for Correspondence: ab72@njit.edu

Robert B Barat
Otto York Department of Chemical Engineering,
New Jersey Institute of Technology, Newark,
New Jersey 07103, United States of America

Zoi-Heleni Michalopoulou
Department of Mathematical Sciences, New Jersey Institute of Technology, Newark, New Jersey 07102,
United States of America

Abstract—Interferometric imaging is a non-invasive, non-contact method to detect concealed lethal agents employing spectral imaging in the terahertz (THz) range. Parallel to the experimental testing over short range, extensive modeling simulates reconstructed images of lethal agents at different frequencies applying interferometric techniques. Near-field correction to such imaging has been accounted for and edge probe algorithm and consequent artificial neural network analyses identify the agents under consideration. This work addresses the issues related to THz imaging for rapid and successful recognition of lethal agents in security screening.

Index Terms—Terahertz imaging, interferometric arrays, artificial neural networks, kohonen self organizing maps, detection of concealed agents

I. INTRODUCTION

In the wake of the acute sense of vulnerability to concealed threats, a primary focus of national security is to develop non-obtrusive, yet highly reliable schemes, for monitoring and detection of different lethal agents. Lying between the microwave and infrared region of the electromagnetic spectrum between 0.1-10 THz, terahertz radiation bridges the gap between photonic and electronic devices and offers a large expanse of unused, unexplored bandwidth. Its ability to penetrate non-metallic common materials, such as clothing, plastic, ceramic, wood, and identify hidden objects, such as plastic explosives, chemicals and other materials beneath clothing and in packages[1,2,3], presents an opportunity to use THz technology in the areas of security and defense. In future, therefore it can be expected that, THz technology would be able to complement and enhance existing and emerging techniques to increase operational effectiveness in the areas of security screening [4,5,6].

In the present study, a novel screening method has been discussed as shown in Figure 1, which combines the spectral imaging capability of THz waves through characteristic

transmission or reflection spectrum of explosive agents[7] and interferometric imaging technique[8] which provides spatial detection of such lethal agents using only a few number of detectors. In addition to the experimental testing[9] of this THz imaging system, extensive simulation yields spatial composite images of agents at different frequencies, providing spectral contrast. These images are simulated based on the spectral data obtained in THz time domain spectroscopic system and different interferometric detector configurations. The consequent processes of artificial neural network (ANN) analyses, to achieve positive identification of lethal agents out of the composite images, are carried out using two distinct methodologies, namely the Multilayer Perceptron (MLP) model and Kohonen Self Organizing Map (KSOM).

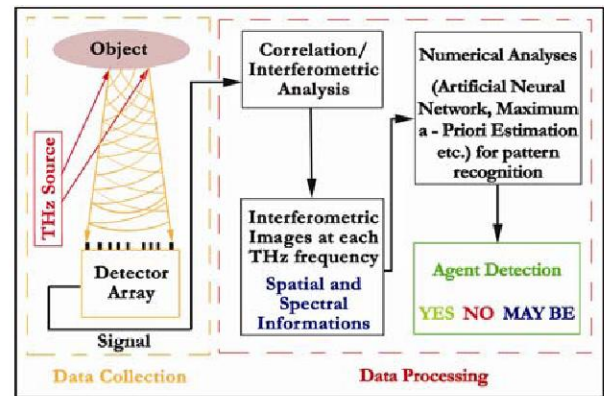


Fig.1(Color online) Proposed THz imaging system for security screening

II. INTERFEROMETRIC THz IMAGING

The proposed imaging interferometer consists of an array of individual detectors arranged non-periodically. As the wavefront of reflected (or transmitted) THz radiation encounters the array, each pair of detectors measures one spatial Fourier component of the incoming THz radiation as determined by the separation of the detector pair, otherwise known as a base line. In order to obtain an interferometric

image of an object by an N element detector array, measurement of amplitudes and phases of THz field at the point of each element are necessary and for a linear set of N

$$\sigma_E(\xi) = \sum_{i=1}^{N(N-1)/2} [\text{Re}(C(u_i)) \cos(2\pi u_i \xi) - \text{Im}(C(u_i)) \sin(2\pi u_i \xi)] \quad (1)$$

where for detector positions x_m and x_n we have $u_i = (x_n - x_m) / \lambda$ and $C(u_i) = A_i e^{i\Delta\phi_i}$, where $A_i = E_m E_n$ and $\Delta\phi_i = \phi_m - \phi_n$ represent the product of electric field amplitudes and change in phase for each baseline pair combination, respectively.

In the present experiment, only one THz detector was used, which was mounted on an X-Y computer controlled stage. The movement of this stage allows the change in the position of the THz detector and obtains oscillations of THz field at several points. Subsequent extractions of the THz amplitude and phase at those points from the obtained data are done to obtain the electric field correlation function for each pair of detector positions resulting in the image reconstruction using the interferometric imaging method.

Unlike the astronomical applications where the interferometric imaging array is typically operated in the far field, for the stand-off detection applications, the object to be imaged is in the near-field region of the imaging array. Consequently, the far-field image reconstruction must be modified to account for the curvature of the wave fronts (that is, the spherical wavefront) in the near-field. To obtain the measure of the performance of the proposed THz imager, we first image a point source of THz radiation for a particular detector configuration, which essentially provides the point spread function or the impulse response function of the detector array. Figure 2 shows the comparison between the reconstructed line THz images of a point THz source with near-field correction with theoretical predictions of a point source image. The near-field correction is calculated conceptually by repositioning the detectors from a linear arrangement to a spherical arrangement that matches the curvature of the incoming wavefront. The interferometric array in this case was of 8 detectors at a distance of 40.9 cm from the source.

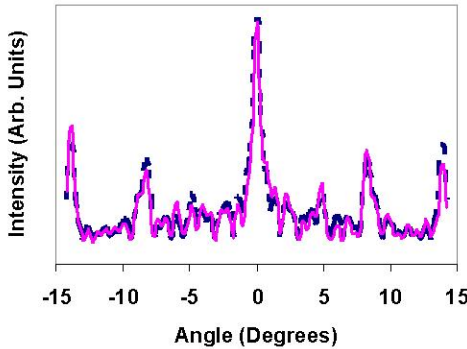


Fig. 2(Color online) Comparison of a reconstructed line image (solid line) with near-field correction and theoretically predicted point image (dashed).

detectors, the image formed is represented by the brightness distribution[10], given by

Subsequently, a piece of 3 cm wide rough metal object is imaged using the same detector configuration at a distance of ~ 1 m. The object surface is kept rough which provides uncorrelated reflections of electric field from the object. Figure 3 shows a linear interferometric image of the metal object without (top) and with (bottom) a barrier of book bag, respectively. Behind the bag, object is still detected at the correct position. The book bag used in the experiment is ~ 2 mm thick and is non-transparent for visible light.

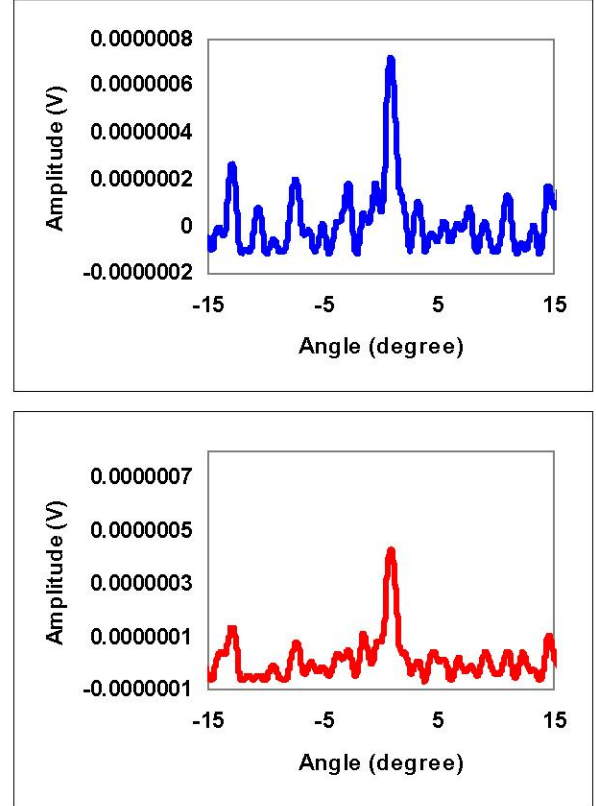


Fig. 3(Color online) Linear interferometric images of a metal object obtained with reflected THz radiation, where (top) shows the image of the metal object (no barrier) and (bottom) the image of the same object hidden behind a book bag.

III. INTERFEROMETRIC IMAGING SIMULATIONS

Due to the current limitation in the availability of resources, especially in terms of suitable THz sources and detectors, the measure of the performance of the proposed THz imager are also estimated through extensive simulations using spatial composite images of agents at different THz frequencies. These images are simulated based on the spectral data obtained with a THz Time Domain Spectroscopic (THz-TDS) system and different interferometric detector configurations.

For the interferometric image simulation, the starting point is a bitmap image of the object under study. The image is then appropriately converted to multiple images at different THz frequencies, containing the spectral characteristics of different elements present, based on their individual THz reflection spectra. After the Fourier transform of these raw images, they are multiplied by the corresponding Fourier transform of the mask at those frequencies. These masks are the impulse response or the point spread function for the imaging system. They are dependent on specific detector configuration, and the distance between the object and detector plane. In other words, these functions are the measure of the energy spread of a central THz source as measured by the specific detector array placed at a certain distance. The product of these two functions upon inverse Fourier transform produces the reconstructed interferometric images of the object under study at those particular THz frequencies.

In the present study, we consider an object “Metal-RDX” which consists of a 1 inch disc of gold mirror and a 1 inch disc of Composite C 4 placed 2 inches apart at a distance of 39 inches or ~ 1 m from the detector array. The detector array is linear and has 10 detectors and the probing frequencies are 0.7 THz and 0.9 THz which are found to be producing a contrast of roughly 8% for Composite C 4 in its reflection spectrum as measured with the THz Time Domain experimental set-up[11]. This contrast can be observed in Figure 4 which shows the simulated interferometric reconstructed images of the object “Metal-RDX”.

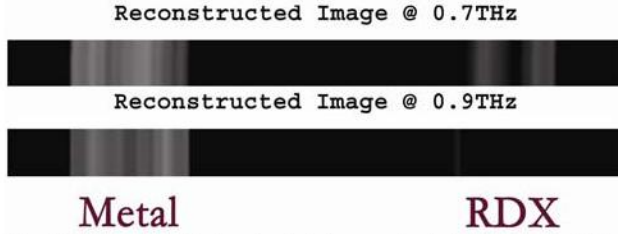


Fig. 4(Color online) The simulated reconstructed images of “Metal-RDX”

IV. ARTIFICIAL NEURAL NETWORK ANALYSES

Interferometric reconstructed images obtained either from experimental observation or through simulation, cannot be interpreted directly to make any identification of agents. These images contain the characteristic fringe pattern of the interferometric image formation apart from additional effects due to noise, fluctuation and other variables. Therefore the spatial and spectral information about various agents present in the images are essentially intractable using traditional numerical approaches. Therefore, towards the realization of accurate classification and positive identification of lethal and non-lethal groups of elements in an image, Artificial Neural Network (ANN) analyses are employed.

ANN is essentially a computing architecture for solving problems of classification, pattern recognition and identification. ANN is extensively used in various industrial, business and scientific applications [12]. Incidentally, the first

widely reported commercial application of neural networks outside the financial industry was in the area of security screening in 1989[13]. In contrast to its traditional counterpart such as the statistical technique or discriminant analysis, ANN has the ability to adapt to the effects of multiple variability by processing sufficiently large datasets to optimize an error criterion and faster performance owing to its tremendous number of interconnects and simple processors[14]. There are various types of ANN architectures frequently used in the application of image processing and pattern recognition [15]; in our present study, we adopted two specific types, namely the Multilayer Perceptron (MLP) model and Kohonen Self Organizing Maps (KSOM).

Multilayer Perceptron model performs the task of pattern classification through supervised learning. As shown in Figure 5, once trained, this model successfully identifies the explosive agent in the presence of metal out of the simulated reconstructed images shown in Figure 4.

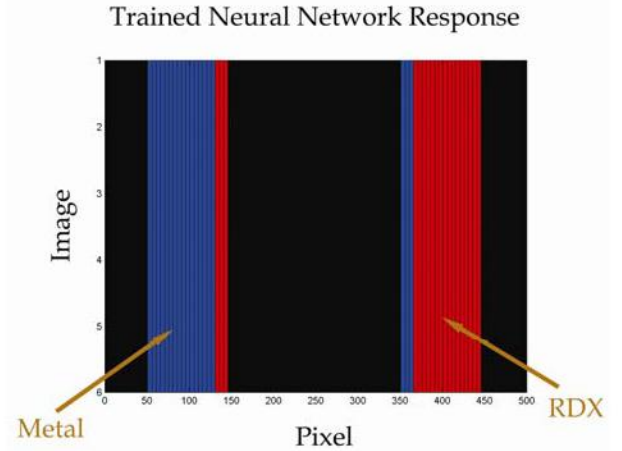


Fig. 5 (Color online) Trained Multi Layer Perceptron Model response

In the above figure, it can be seen that, in some of the pixel positions in between the metal and RDX discs, some ambiguities are found. This is a fundamental problem of digital image processing[16], simply known as boundary effect. When the sampling function chooses a pixel near to the edge or boundary of an image, then some of the weights of the function also operate upon “invalid pixels” beyond the boundary of the real image. As a result, the intensity values which directly correspond to the spectral characteristics of the agents under concern get distorted near the edge or the boundary of an object and therefore, the MLP cannot classify or discriminate these pixel positions accurately.

Kohonen Self Organizing Maps (KSOM) are neural networks that map input patterns to different regions of a two dimensional space. Figure 6 shows the response of a KSOM to the identical problem of classifying the simulated reconstructed images of “Metal-RDX”.

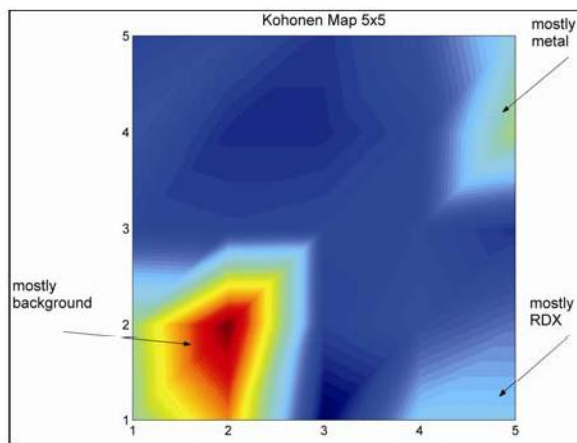


Fig. 6(Color online) Kohonen Self Organizing Map response

KSOM networks do not require training and process input data vectors by calculating measures of distance between them. Vectors with short distances are mapped to the same or neighboring nodes of the map. The process is repeated for several iterations until the map reaches a state of equilibrium. These type of networks are, therefore, inherently more flexible to adapt to different classes of materials for practical purpose, than MLP model which requires extensive training for successful identification.

V. CONCLUSIONS

In this study, we have successfully demonstrated interferometric THz imaging and its potential use in security screening type of application. However, one important disadvantage of linear imaging in our current experimental set-up is that it does not allow the reconstruction of the geometrical shape of the target but only its position. Therefore, the experimental work in progress aims to produce stand-off two dimensional images of extended objects, especially behind barriers at a faster capturing rate. The current challenges of the signal processing are to incorporate statistical nature of noise and the effect of barriers in the image analysis.

REFERENCES

- [1] D. J. Cook, B. K. Decker, G. Maislin, & M. G. Allen, Through container THz sensing: applications for explosives screening. *Proc. SPIE*. **5354**, 55–62 (2004)
- [2] K. Kawase, Y. Ogawa, & Y. Watanabe, Non-destructive terahertz imaging of illicit drugs using spectral fingerprints. *Opt. Exp.* **11**, 2549–2554 (2003)
- [3] D. A. Zimdars, & J.S. White, Terahertz reflection imaging for package and personnel inspection. *Proc. SPIE*. **5411**, 78–83 (2004)
- [4] M.C. Kemp, et al. Security applications of terahertz technology. *Proc. SPIE*. **5070**, 44–52 (2003)
- [5] M. K. Choi, A. Bettermann, & D. W. Van der Wiede, Potential for detection of explosive and biological hazards with electronic terahertz systems. *Phil. Trans. R. Soc. Lond. A* **362**, 337–349 (2004)
- [6] D. M. Mittleman, et al. Recent advances in terahertz imaging. *Appl. Phys. B*. **68**, 1085–1094 (1999)
- [7] J. F. Federici, et al. THz imaging and sensing for security applications - explosives, weapons, and drugs. *Semicond. Sci. Technol.* **20** S266–S280 (2005)
- [8] J. F. Federici, et al. Terahertz imaging using an interferometric array. *Appl. Phys. Lett.* **83**, 2477 (2003)
- [9] A. Bandyopadhyay, et al. Terahertz interferometric and synthetic aperture imaging. *J. Opt. Soc. Am. A* "In Press"
- [10] J. F. Federici, et al. Terahertz near-field interferometric and synthetic aperture imaging, in *Terahertz for Military and Security Applications*, R. J. Hwu & D. L. Woolard, eds., *Proc. SPIE*. **5411**, 9–17 (2004)
- [11] A. Sengupta, A. Bandyopadhyay, R. B. Barat, D. E. Gary & J. F. Federici, "THz reflection spectroscopy of Composition C 4 and its detection through interferometric imaging," in *THz and GHz Electronics and Photonics V*, R. J. Hwu ed., *Proc. SPIE* **6120** (In Press)
- [12] B. Widrow, D. E. Rumelhart & M. A. Lehr, "Neural Networks: Applications in industry, business and science," *Communication of the ACM*, **37**, 93–105 (1994)
- [13] P. M. Shea & V. Lin, "Detection of explosives in checked airline baggage using an artificial neural system," in *Proceedings of IEEE International Joint Conference on Neural Networks* (Institute of Electrical and Electronics Engineers, New York, 1989), pp. 31–34
- [14] J. E. Dayhoff. *Neural Network Architectures: An Introduction* (Van Nostrand Reinhold, New York, 1990)
- [15] C. T. Leondes, eds. *Image Processing and Pattern Recognition* (Academic Press, San Diego, 1998)
- [16] G. J. Awcock & R. Thomas. *Applied Image Processing*. (McGraw-Hill Inc., New York, 1996)